The hepatocyte epidermal growth factor receptor (EGFR) pathway regulates the cellular interactome within the liver fibrotic niche

E Gonzalez-Sanchez, J Vaquero *et al. J Pathol* https://doi.org/10.1002/path.6299

Supplementary materials and methods
Supplementary Figures S1–S11
Supplementary Tables S1–S5

Reference numbers refer to the main text list

Supplementary materials and methods

In vivo *experimental procedures* (*additional information*)

Wild-type (WT) and ΔEGFR mouse lines were maintained in a C57BL/6 background in the UCM animal facility and allowed food and water *ad libitum* in temperature-controlled rooms under a 12 h light/dark cycle, and routinely screened for pathogens in accordance with Federation of European Laboratory Animal Science Associations procedures. All animal procedures conformed to ARRIVE Guidelines and European Union Directive 86/609/EEC and Recommendation 2007/526/ EC, enforced in Spanish law under RD 1201/2005. Animal protocols including sample size decisions and randomization and blinding strategies were approved by the Animal Experimentation Ethics Committee of the UCM and the Animal Welfare Division of the Environmental Affairs Council of the Government of Madrid (Proex 262.6/21). We have followed the 3R recommendations: Replacement, Reduction, and Refinement. To avoid potential bias, experimental groups included animals from litters coming from different breedings. Furthermore, littermates included mice treated with mineral oil and CCl_4.

Histological and immunohistochemical analyses

Liver sections (3- to 10-μm thick) were cut from paraffin-embedded blocks. Hematoxylin and eosin staining and immunohistochemical analyses were performed as described previously [12]. Liver sections were stained with picro-sirius red to evaluate collagen

deposition and therefore fibrosis. Primary antibodies (listed in supplementary material, Table S1) were incubated overnight at 4 °C and binding was detected using a Vectastain ABC kit (Vector Laboratories, Burlingame, CA, USA). Nuclei were stained with hematoxylin solution and preparations were mounted in DPX. Stained sections were visualized using a Nikon Eclipse 80i microscope coupled to a Nikon DS-Ri1 digital camera or scanned on a virtual slide scanner NanoZoomer 2.0 HT (Hamamatsu, Tokyo, Japan) at the Histopathology Facility of the Institute for Research in Biomedicine – IRB (Barcelona, Spain). Morphometric analyses were performed blinded, using ImageJ analysis software (National Institutes of Health, Bethesda, MD, USA).

In parallel, serum levels of the hepatocellular damage markers aspartate aminotransferase (AST) and alanine aminotransferase (ALT) were measured in the Echevarne Laboratories (Barcelona, Spain).

Isolation of hepatic non-parenchymal cells for immune cell population analysis

Livers were collected and washed with PBS, and then immediately transferred to HBSS (Hank's Balanced Salt Solution; Gibco, Life Technologies, Carlsbad, CA, USA) at room temperature, disintegrated, and filtered through 100-µm cell strainers. Then homogenates were centrifuged at 500 × *g* for 5 min at room temperature, and cell pellets were resuspended in a 36% Percoll solution (GE Healthcare Bio-Sciences AB, Uppsala, Sweden) containing 100 UI/ml heparin (HIBOR 5000 UI; ROVI, Madrid, Spain). After centrifugation at 800 × *g* (without a brake) for 20 min at room temperature, supernatants were discarded and then erythrocytes were removed from cell pellets by using a red blood cell lysis buffer (150 mM NH_4Cl, 10 mM $KHCO_3$, 0.1 mM EDTA, pH 7.3). The resulting cell pellets were washed with cold HBSS, centrifuged at 500 × *g* for 5 min at 4 °C, and finally, cells were resuspended in cold HBSS for further analysis. Isolated non-parenchymal liver cells were incubated with the antibodies listed in supplementary material, Table S2, or their corresponding isotype controls for 20 min at room temperature protected from light. After washing steps, cells were resuspended with PBS. Flow cytometry data were acquired using a FACSCanto II (BD Biosciences, Erembodegem, Belgium) and data analysis was performed using Cytomics FC500 (Beckman Coulter Life Sciences, Miami, FL, USA) with the CXP program.

Analysis of gene expression by RT-qPCR

Levels of mRNA for cell type markers, pro-/anti-inflammatory factors, and genes involved in collagen homeostasis were analyzed by reverse transcription-quantitative PCR (RT-qPCR). Total RNA was isolated from the different cells or tissues using an RNeasy Mini Kit (QIAGEN, Hilden, Germany). cDNA was produced using a High-Capacity cDNA Reverse Transcription Kit (Applied Biosystems, Waltham, MA, USA). Real-time qPCR was performed in duplicate in a LightCycler® 480 Real-time PCR system (Roche Diagnostics GmbH, Mannheim, Germany) following the manufacturer's protocol. SYBR Green PCR Master Mix was used for PCR reactions (Applied Biosystems). Primers are listed in supplementary material, Tables S3 and S4.

RNA sequencing (*RNA-seq*) *analysis of hepatocytes*

Primary mouse hepatocytes were isolated as described previously [38]. Livers from 2- to 3-month-old male mice were perfused with HBSS supplemented with 10 mM HEPES and 0.2 mM EGTA for 5 min, followed by a 15-min perfusion with William's Medium E containing 10 mM HEPES and 0.03% collagenase type 1 (125 U/mg; Worthington Biochemical Corp., Lakewood, NJ, USA). Livers were further minced, filtered through a 70-µm cell strainer (BD Biosciences, Franklin Lakes, NJ, USA), and viable hepatocytes were selected by centrifugation in Percoll and stored at –80 ºC. Total RNA from mice was quantified using a Qubit® RNA BR Assay Kit (Thermo Fisher Scientific, Bremen, Germany), and the RNA integrity was estimated by using an RNA 6000 Nano Bioanalyzer 2100 Assay (Agilent, Santa Clara, CA, USA). The RNA-seq libraries were prepared using a KAPA Stranded mRNA-Seq Illumina® Platforms Kit (Roche, Indianapolis, IN, USA) following the manufacturer's recommendations, starting with 500 ng of total RNA as the input material. The library was quality-controlled on an Agilent 2100 Bioanalyzer using a DNA 7500 assay. The libraries were sequenced on a NovaSeq 6000 (Illumina) with a read length of 2 × 151 bp, following the manufacturer's protocol for dual indexing. Image analysis, base calling, and quality scoring of the run were processed using the manufacturer's software Real Time Analysis (RTA 3.4.4). RNA-seq reads were mapped against the *Mus musculus* reference genome (GRCm39) using STAR aligner version 2.7.8a [39] with ENCODE parameters. Annotated genes were quantified using RSEM version 1.3.0 [40] with default parameters, using the annotation file from GENCODE version M31. Differential expression analysis was

performed using the limma v3.4.2 R package, with TMM normalization. The voom function [41] was used to estimate mean-variance relationship and to compute observation-level weights. The linear model was fitted with the voom-transformed counts and contrasts were extracted. Genes were considered differentially expressed (DEG) with adjusted *p* value <0.05, and subsets of DEGs were represented in heatmaps using the pheatmap R package, with voom-transformed counts scaled by row. A functional enrichment analysis was performed on the DEGs using gprofiler2 v0.1.8 [42], using ENSEMBL databases as reference. Additionally, a gene set enrichment analysis (GSEA) was performed with the list of pre-ranked genes by a *t*-statistic using the R package fgsea v1.12.0 (https://pubmed.ncbi.nlm.nih.gov/16199517/) against the mouse Reactome database and M5 gene set collection from MSigDB.

Additionally, specific TGF-β signaling and EMT gene signatures were deconvoluted from $\log_2$ TPM expression data using gene set variation analysis (GSVA) [43] and tested using Kruskal–Wallis tests.

In vitro *analyses*

Immortalized hepatocytes were isolated from ΔEGFR or WT mice as described previously [12]. Hep3B human hepatocarcinoma and THP-1 human monocyte cell lines were obtained from the European Collection of Cell Cultures (UK Health Security Agency, Porton Down, Salisbury, UK), whereas the RAW 264.7 mouse macrophage cell line was kindly provided by Dr Nicolas Chignard (CRSA, Paris, France). Cells were cultured with DMEM medium supplemented with 10% (v/v) heat-inactivated FBS, 100 U/ml penicillin, and 100 µg/ml streptomycin, maintained in a humidified atmosphere of 37 °C, 5% CO_2, and routinely screened for the presence of mycoplasma. Conditioned media were prepared as follows: murine immortalized hepatocytes or Hep3B cells were seeded and 24 h later, serum-starved overnight. The cells were then treated with heparin binding EGF-like growth factor (HB-EGF, an EGFR ligand) at a concentration of 20 ng/ml. PBS was used as vehicle. After 30 min, the cells from one plate of each cell line and experimental condition were collected for control studies to validate the activation of the EGFR pathway. Two hours after the treatment, the medium was replaced by FBS-free medium in the absence of the EGFR ligand. The conditioned media were collected 24 h later and used to analyze their effects on RAW 264.7 mouse macrophages or THP-1 human monocytes. Gene expression was

determined using RT-qPCR and RAW 264.7 and THP-1 monocytes after 48 h incubation with conditioned medium collected from murine immortalized hepatocytes or Hep3B cells, respectively. In the case of THP-1 monocytes, the effect of conditioned medium from Hep3B cells on cell adhesion was evaluated after 24 h of exposure using the xCELLigence System (Agilent), with phorbol myristate acetate (PMA) as a positive control.

Western blot analysis

Western blotting was performed as described previously [44]. In brief, tissue and cells were lysed in RIPA lysis buffer supplemented with orthovanadate and a cocktail of protease inhibitors at 4 °C [using a TissueLyser (QIAGEN) to homogenize liver tissue] and protein concentrations determined using a BCA kit (Pierce, Thermo Fisher Scientific). Proteins were separated by SDS electrophoresis on 10% polyacrylamide gels, then transferred to nitrocellulose membranes. Membranes were incubated with the primary antibodies (supplementary material, Table S1) overnight at 4 °C and then with ECL Mouse IgG and Rabbit IgG, HRP-Linked antibodies (GE Healthcare, Buckinghamshire, UK) (1/2,000) for 1 h at room temperature. Blots were visualized using a ChemiDoc™ Touch Imaging System (Bio-Rad Inc., Hercules, CA, USA) and densitometric analysis was performed using Image Lab™ Software (Bio-Rad Inc.).

Proteomic analysis of the secretome

Proteomic analysis of the conditioned media obtained in the *in vitro* experiments was performed in the Proteomics Unit of the Complutense University of Madrid. A label-free experiment was conducted. In brief, secretome samples were concentrated using a speed vac and resuspended in 8 M urea. Proteins were digested using an iST kit (Preomics, Planegg, Germany). The resulting peptides were analyzed using liquid nano-chromatography (Vanquish Neo, Thermo Fisher Scientific), coupled to a Q-Exactive HF high-resolution mass spectrometer (Thermo Fisher Scientific).

Proteins were identified using Proteome Discoverer 3.0 software (Thermo Fisher Scientific) and the search engine Mascot 2.6 (http://matrixscience.com). The database used was Uniprot (UP-000000589). For quantitative proteomics, using the aforementioned software, chromatograms and retention times of all samples were aligned. Afterwards, total protein abundance between different samples was normalized. The differential abundances of proteins between samples were compared.

Data analysis of publicly available human gene expression

The data for the Fujiwara *et al* cohort of liver biopsies from HCC-naïve NAFLD patients were accessed through Gene Expression Omnibus (GEO) accession number GSE193066. Relative log-expression normalized data were directly downloaded from GEO. Two EGFR signaling gene signatures were obtained from MSigDB v2023.1 [45], 'EGF/EGFR signaling' from WikiPathways (C2 CP) and 'EGFR target genes' from TFT (C3), and GSVA [43] was used to assess the relative activation of the signature in the samples.

Correlation, in fibrotic samples, between the EGFR signature and genes of interest was assessed using Pearson's correlation. Kendall's τ was used to assess the association between either EGFR signatures or gene expression with fibrosis stage. All *p* values were adjusted using a Bonferroni correction test. All analyses were performed using R v4.0.4 [46].

Statistical analysis

Statistical analyses have been specified in each of the technologies. Data representation as box and whisker plots was performed using GraphPad Prism software version 5.0 (GraphPad Software Inc., San Diego, CA, USA). Once a normal distribution of data was verified using a Shapiro–Wilk test, differences between groups were compared using Student's *t*-test, or ANOVA, and considered statistically significant when $p < 0.05$.

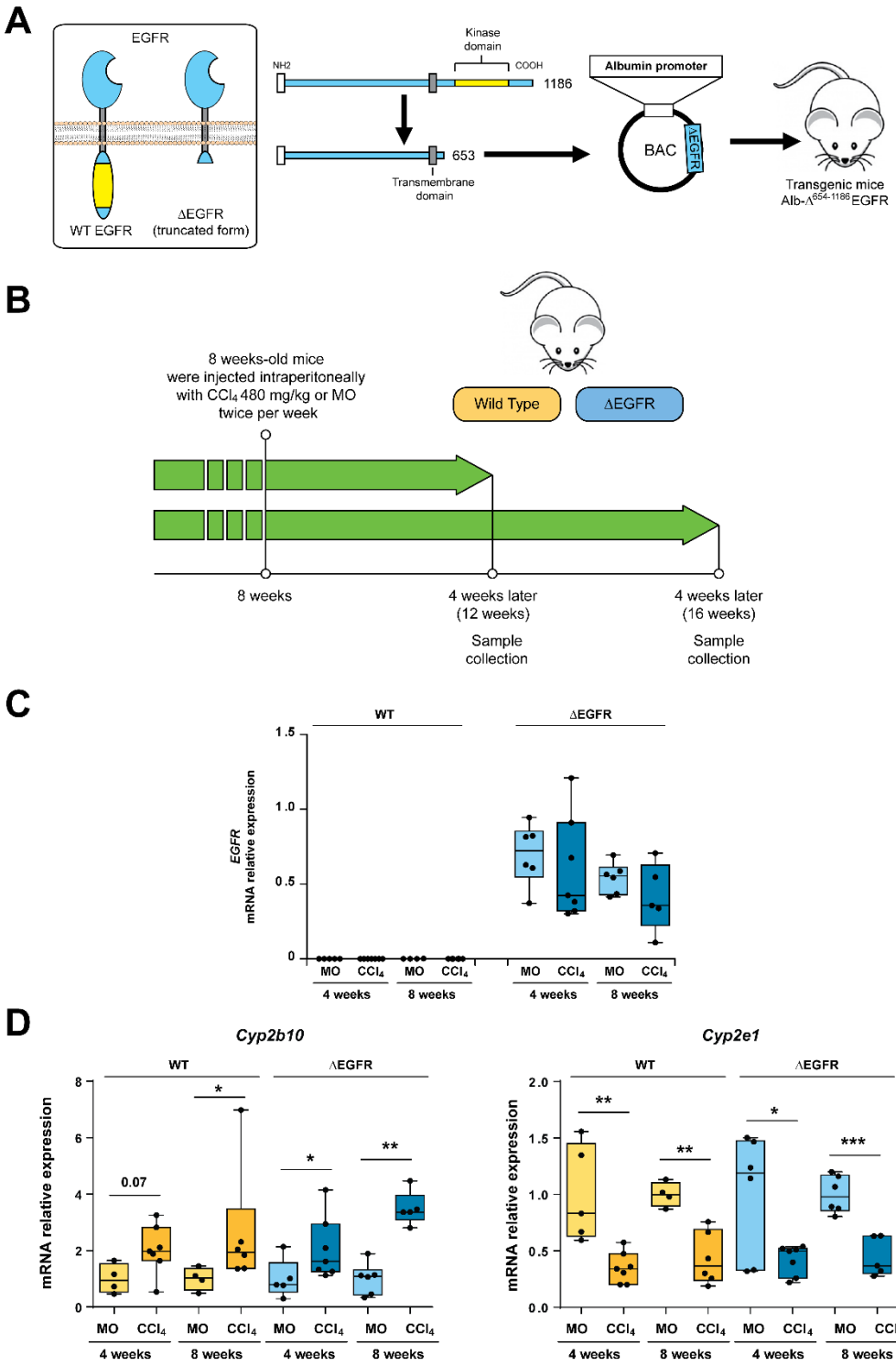

Figure S1. Experimental mouse model. (A) Transgenic model Alb-Δ654-1186EGFR (ΔEGFR) mice. A complementary DNA coding for a truncated form of EGFR with a deletion in its intracytosolic region (amino acids 654–1186) was cloned into a transference plasmid under the control of the albumin promoter locus upstream of the ATG of the mouse albumin gene (*Alb*). (B) Experimental CCl_4-induced liver fibrosis model in WT and ΔEGFR mice. (C, D) Hepatic mRNA expression of human *EGFR* (C) and mouse *Cyp2b10* and *Cyp2e1* (D), determined by RT-qPCR in ΔEGFR and WT mice treated with CCl_4 or mineral oil (MO) for 4 or 8 weeks. Data (n = 4–7 animals per group) were analyzed using Student's t-test. *$p < 0.05$, **$p < 0.01$, versus MO.

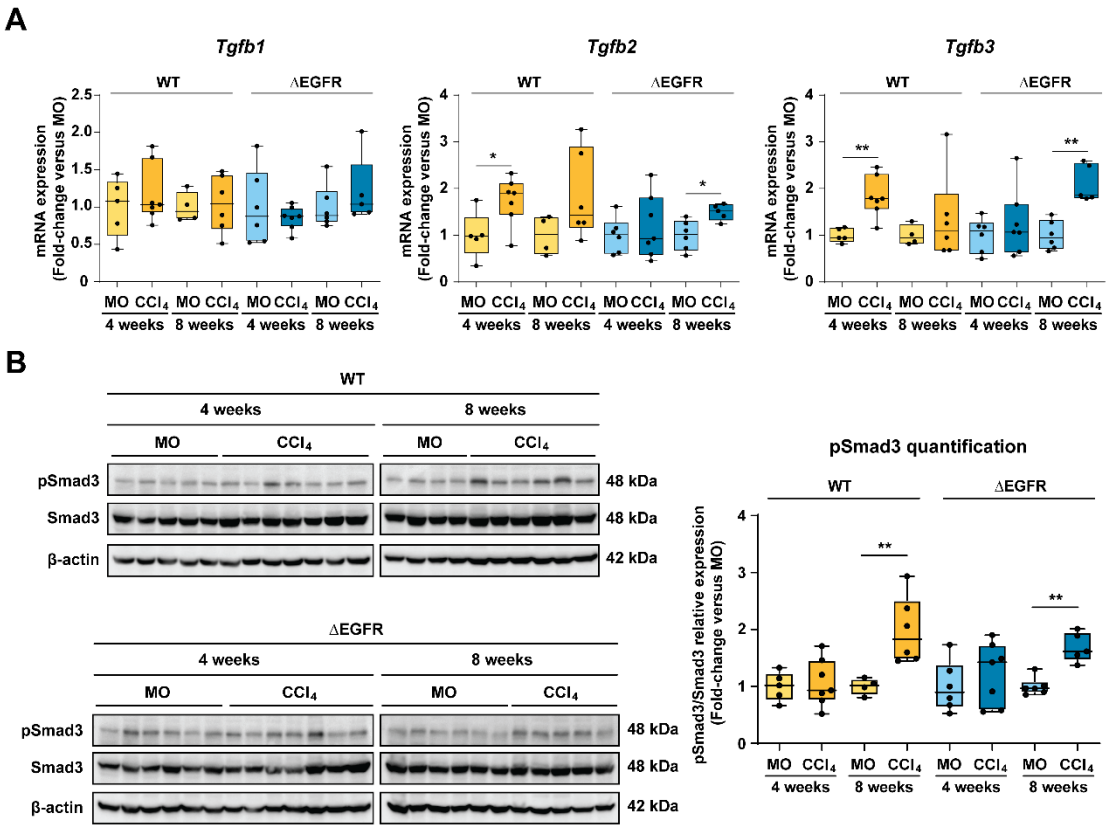

Figure S2. Analysis of the transforming growth factor-beta (TGF-β) pathway in livers from CCl_4-treated ΔEGFR and WT mice. WT and ΔEGFR mice were treated with CCl_4 or mineral oil (MO) for 4 or 8 weeks. (A) The mRNA expression of TGF-β ligands 1–3 (*Tgfb1–3*) was assessed by RT-qPCR. (B) The activation of the signaling pathway was determined by analyzing p-Smad3 protein levels by western blotting, and densitometric quantification of the ratio pSmad3/Smad3 after normalization with β-actin levels. Data (n = 4–7 animals per group) are expressed as fold-change versus MO. *$p < 0.05$, **$p < 0.01$ (Student's t-test).

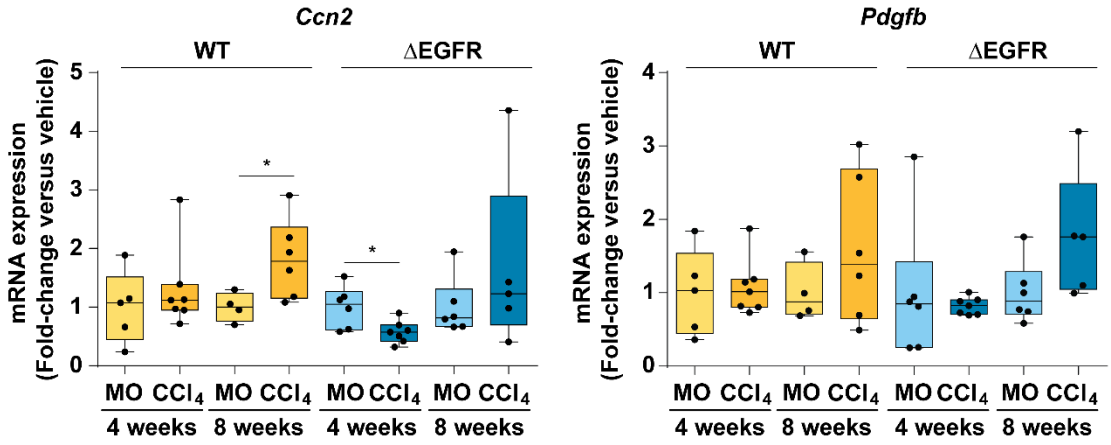

Figure S3. Expression of pro-fibrotic factors in livers from CCl_4-treated ΔEGFR and WT mice. WT and ΔEGFR mice were treated with CCl_4 or mineral oil (MO) for 4 or 8 weeks. The mRNA expression of *Ccn2* and *Pdgfb* was assessed using RT-qPCR. Data (n = 4–7 animals per group) are expressed as fold-change versus MO. *p < 0.05, **p < 0.01 (Student's t-test).

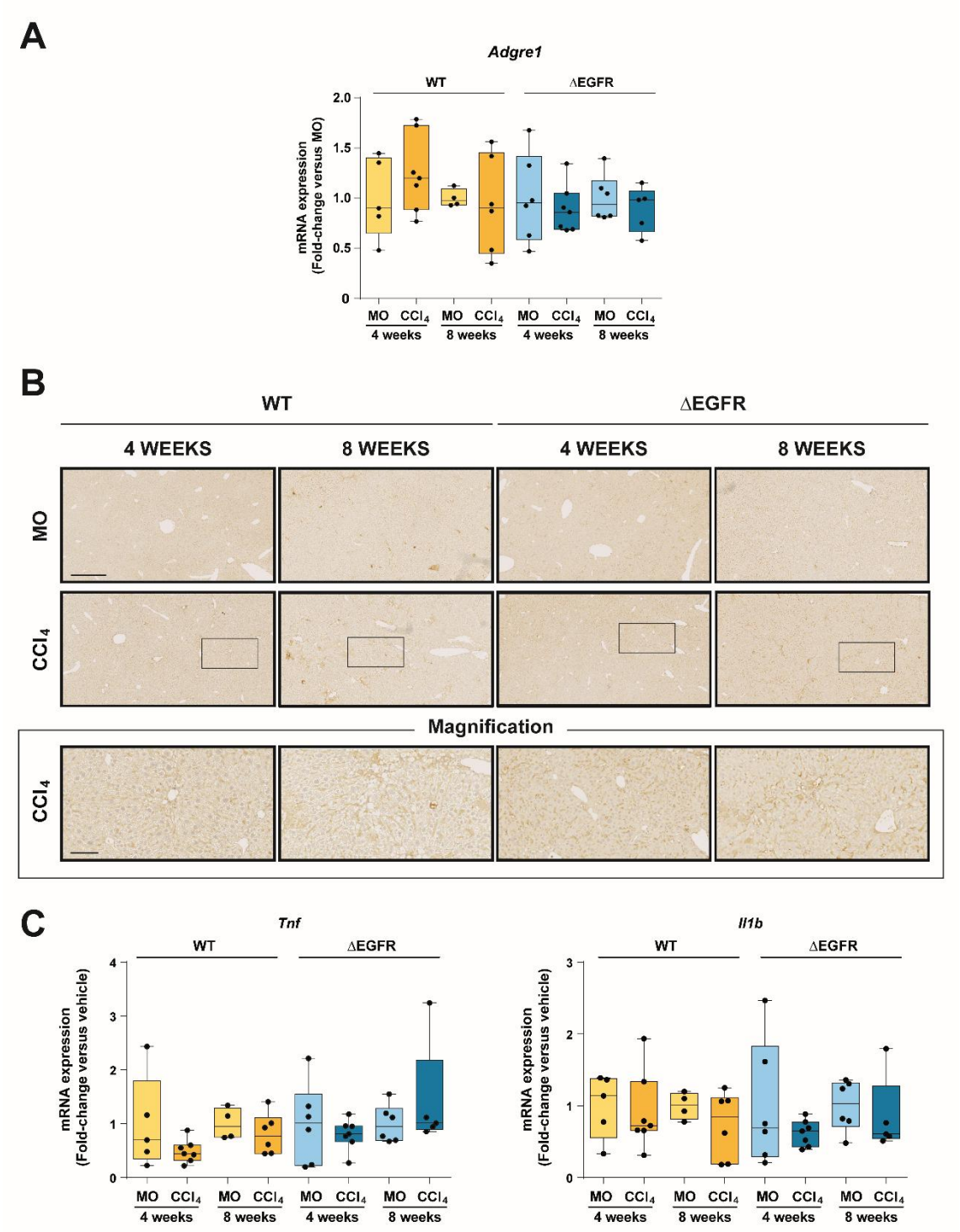

Figure S4. Inflammatory status in livers from CCl_4-treated WT and ΔEGFR mice. WT and ΔEGFR mice were treated with CCl_4 or mineral oil (MO) for 4 or 8 weeks. (A) The mRNA expression of *Adgre1* was assessed by RT-qPCR. (B) F4/80 immunostaining of macrophages. (C) The mRNA expression of *Tnf* and *Il1b* was assessed using RT-qPCR. Data (n = 4–7 animals per group) were analyzed using Student's t-test. Scale bars: 500 µm and 100 µm (magnified views).

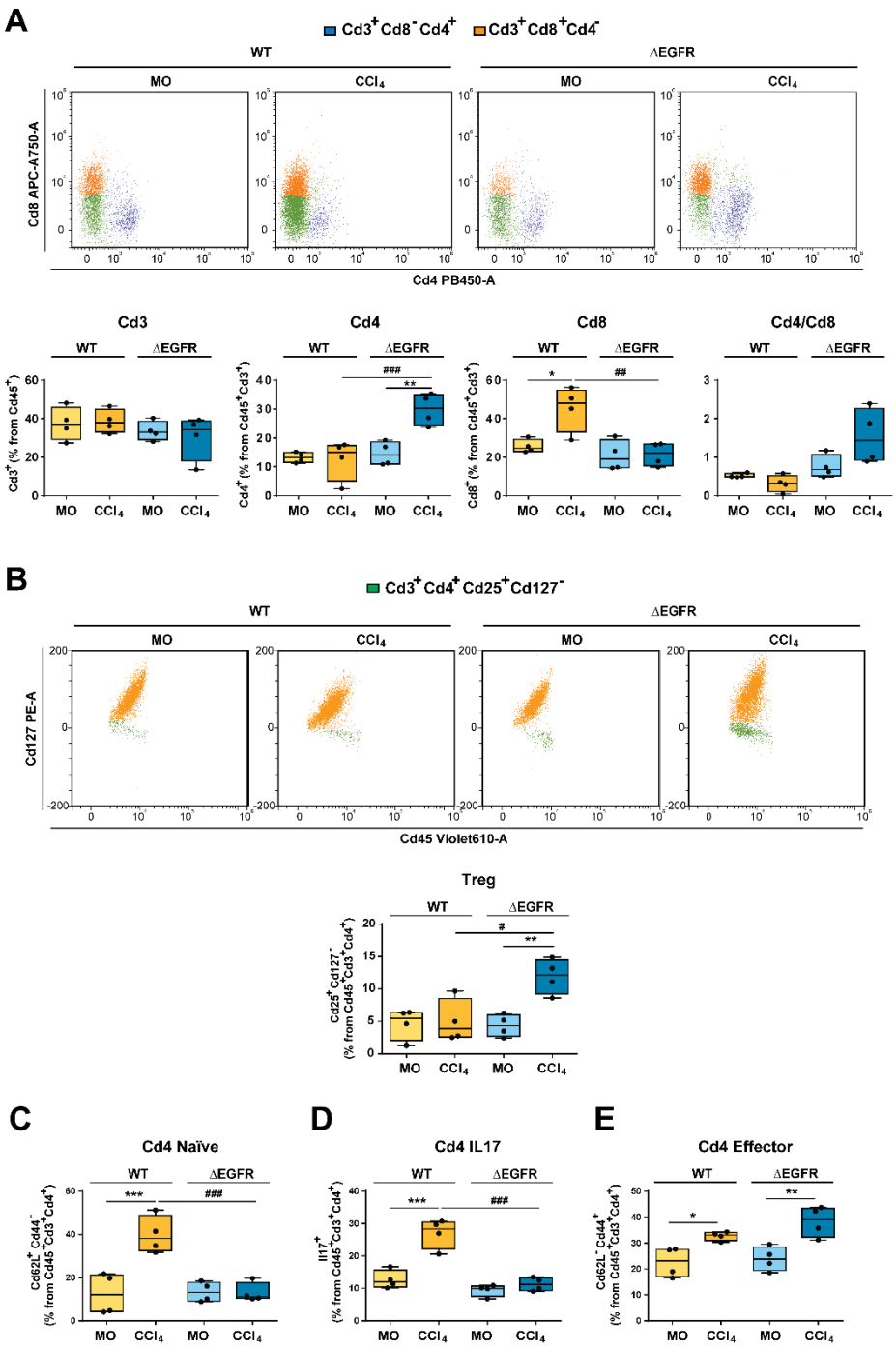

Figure S5. Impairment of the EGFR catalytic activity in hepatocytes alters the lymphocytic infiltrate following CCl_4-induced liver damage. Non-parenchymal liver cells were isolated from WT and ΔEGFR mice after 4 weeks of treatment with CCl_4 (n = 4 animals per group) and analyzed by flow cytometry. (A) $Cd4^+$ and $Cd8^+$ cell populations (Cd4/Cd8 ratio on the right). (B–E) Changes in Cd4 lymphocyte sub-populations: (B) T-reg; (C) Cd4 naïve; (D) Cd4 IL17; (E) Cd4 effector. Data are presented as box and whisker plots. $^{*,\#}p < 0.05$, $^{**,\#\#}p < 0.01$, $^{***,\#\#\#}p < 0.001$ using Student's t-test. *CCl_4 versus vehicle (MO); $^{\#}$ΔEGFR versus WT.

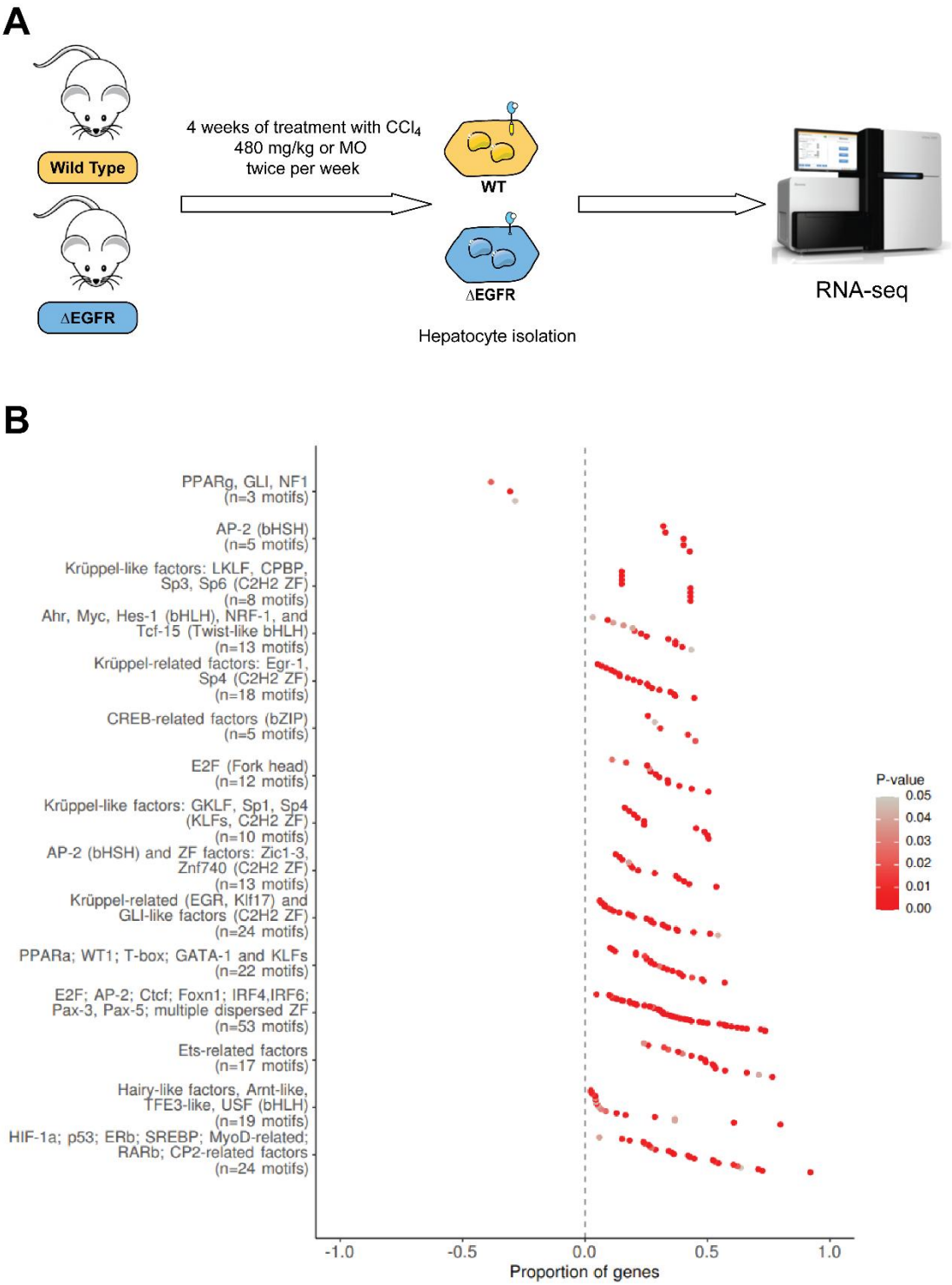

Figure S6. The EGFR pathway regulates the hepatocyte gene transcriptome in response to CCl_4. (A) RNA-seq analysis workflow. Hepatocytes were isolated from WT and ΔEGFR mice treated with CCl_4 or mineral oil (MO) for 4 weeks (*n* = 3 or 4 animals per group). (B) Analysis of enriched transcription factor (TF) activity. Proportion of genes shows the ratio between the set of differentially expressed genes with the total size of genes in the gene set/motif. Dots on the left and right show TF-enriched ΔEGFR and WT, respectively. Significant TF motifs are clustered based on common over-represented genes (over-representation analysis against TRANSFAC database).

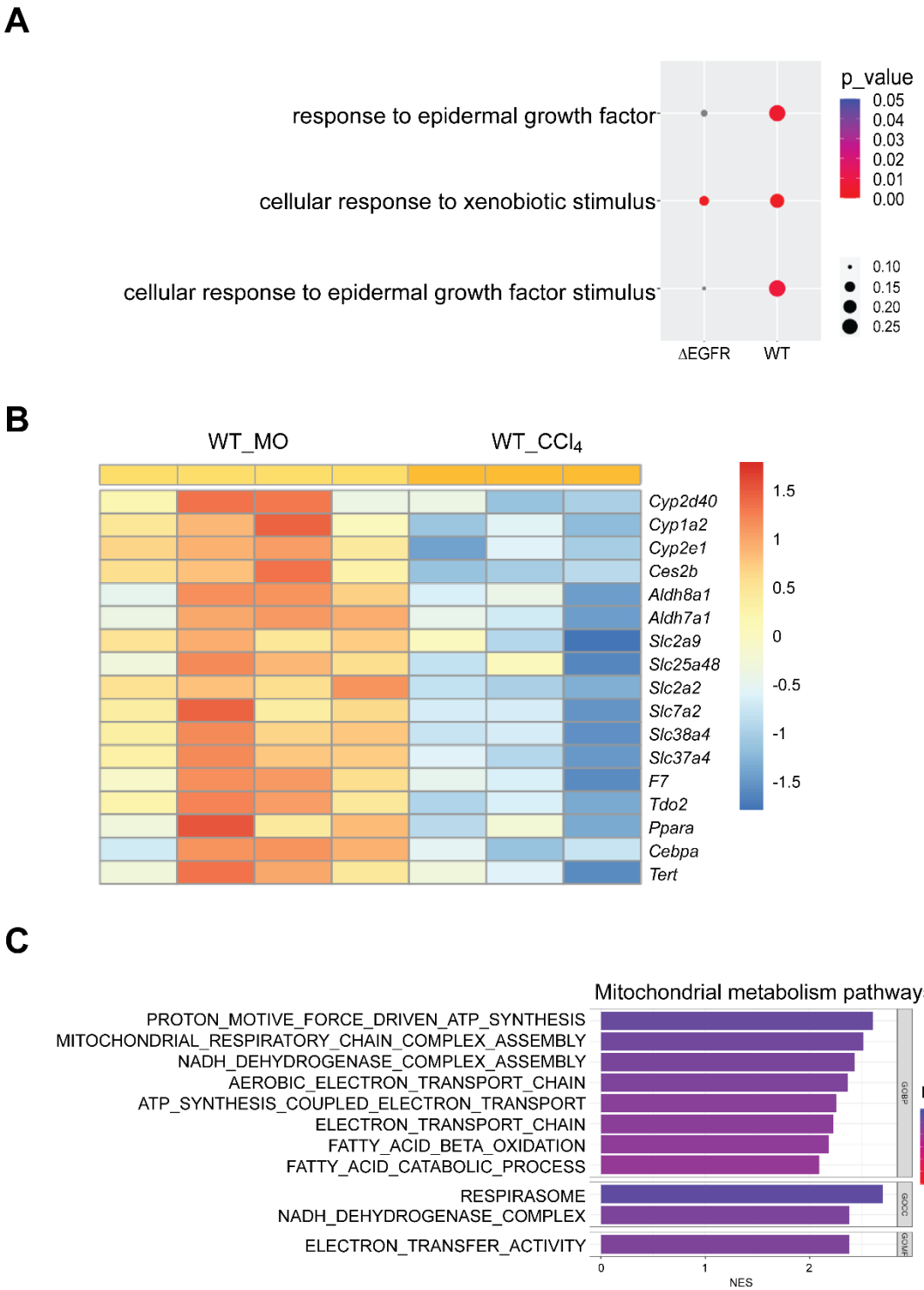

Figure S7. The EGFR pathway regulates the hepatocyte gene transcriptome during the response to CCl_4. (A) Dot plot showing differences in enrichment for key events related to xenobiotic and epidermal growth factor stimulus between WT and ΔEGFR mice. (B) Heatmap showing changes in the expression of genes related to liver-specific functions that appeared specifically in WT hepatocytes, but not in ΔEGFR hepatocytes, after CCl_4 treatment. (C) Bar chart of mitochondrial metabolism pathways that appeared enriched when comparing treated hepatocytes, ΔEGFR versus WT, by GSEA. Data (*n* = 3 or 4 animals per group) were analyzed using pre-ranked GSEA.

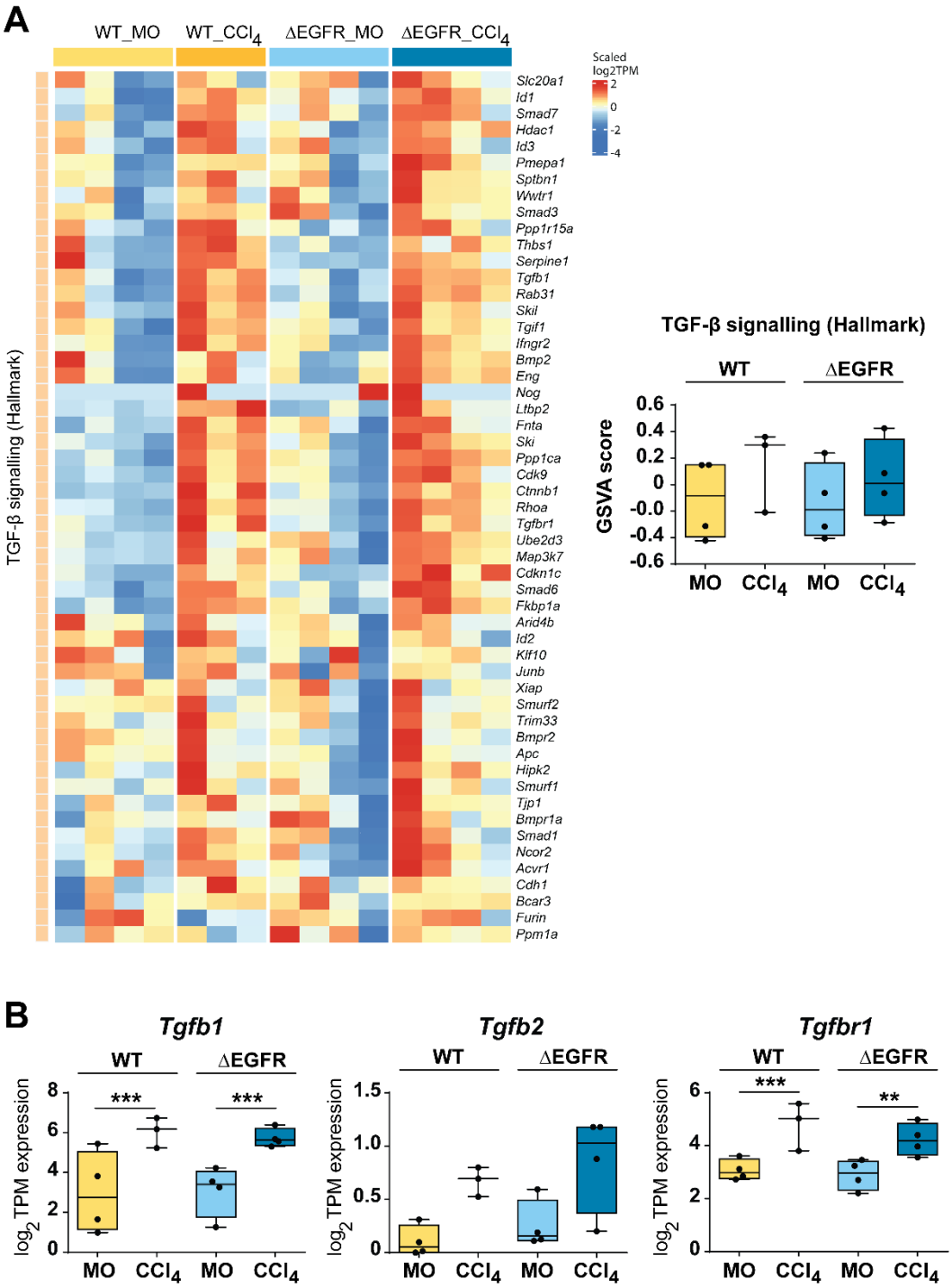

Figure S8. The impairment of EGFR catalytic activity in hepatocytes does not significantly impact the TGF-β pathway during the response to CCl_4. RNA-seq analysis in hepatocytes isolated from WT and ΔEGFR mice treated with either vehicle (mineral oil, MO) or CCl_4 for 4 weeks (4 animals per group, except 3 for WT-CCl_4). (A) Heatmap showing changes in the expression of genes related to TGF-β signaling and gene set variation analysis (GSVA) score. (B) mRNA expression of *Tgfb1*, *Tgfb2*, and *Tgfbr1*, as examples of some of the genes that appeared in the heatmap from A, in hepatocytes from WT *and* ΔEGFR mice (treated with either MO or CCl_4), analyzed by RNA-seq.

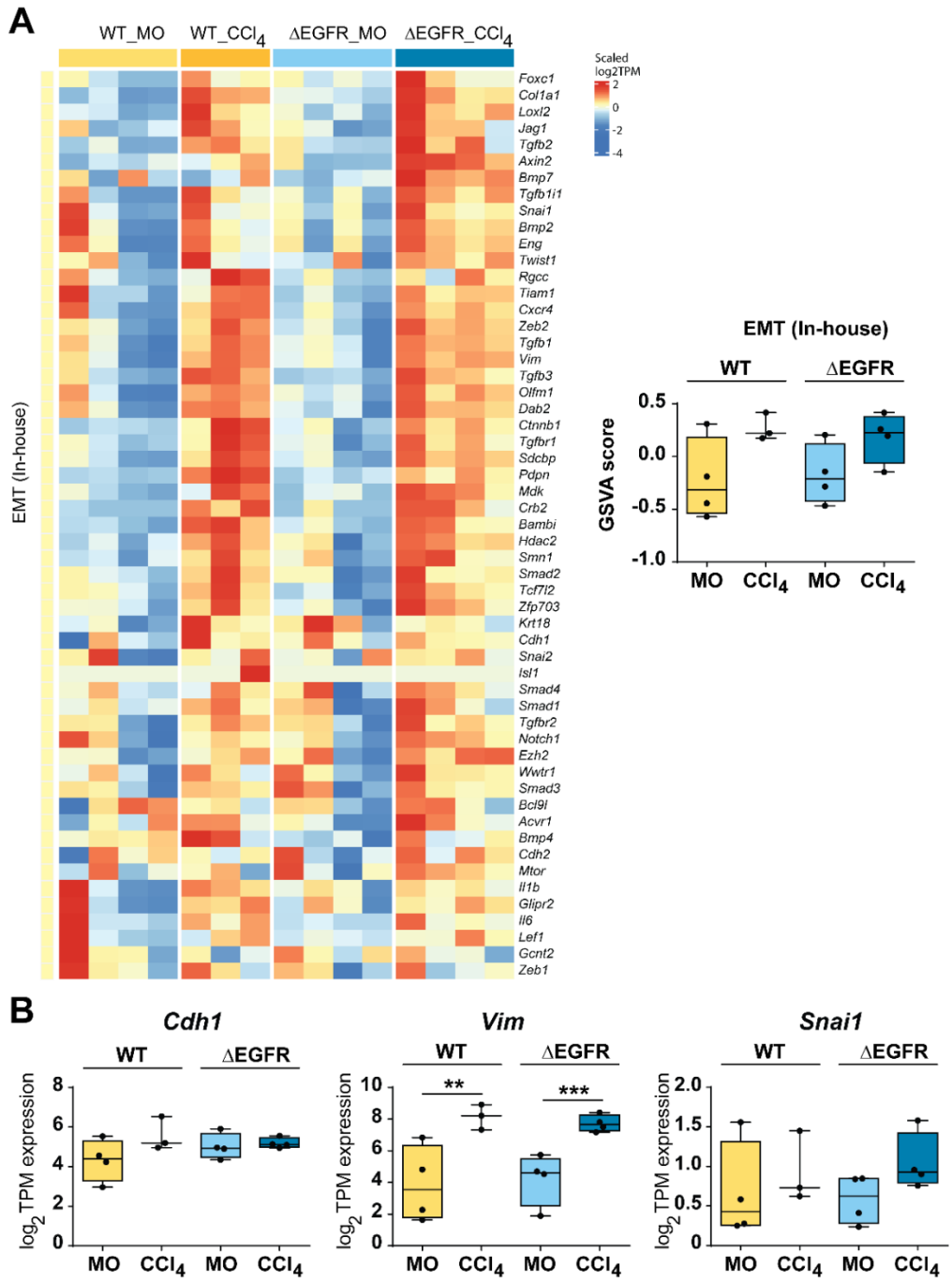

Figure S9. The impairment of EGFR catalytic activity in hepatocytes does not significantly impact the EMT pathway during the response to CCl_4. RNA-seq analysis of hepatocytes isolated from WT and ΔEGFR mice treated with either vehicle (mineral oil, MO) or CCl_4 for 4 weeks (4 animals per group, except 3 for WT-CCl_4). (A) Heatmap showing changes in the expression of genes related to epithelial to mesenchymal transition (EMT) and gene set variation analysis (GSVA) score. (B) mRNA expression of *Cdh1*, *Vim*, and *Snai1*, as examples of some of the genes that appeared in the heatmap from A, in hepatocytes from WT and ΔEGFR mice (treated with either MO or CCl_4), analyzed by RNA-seq.

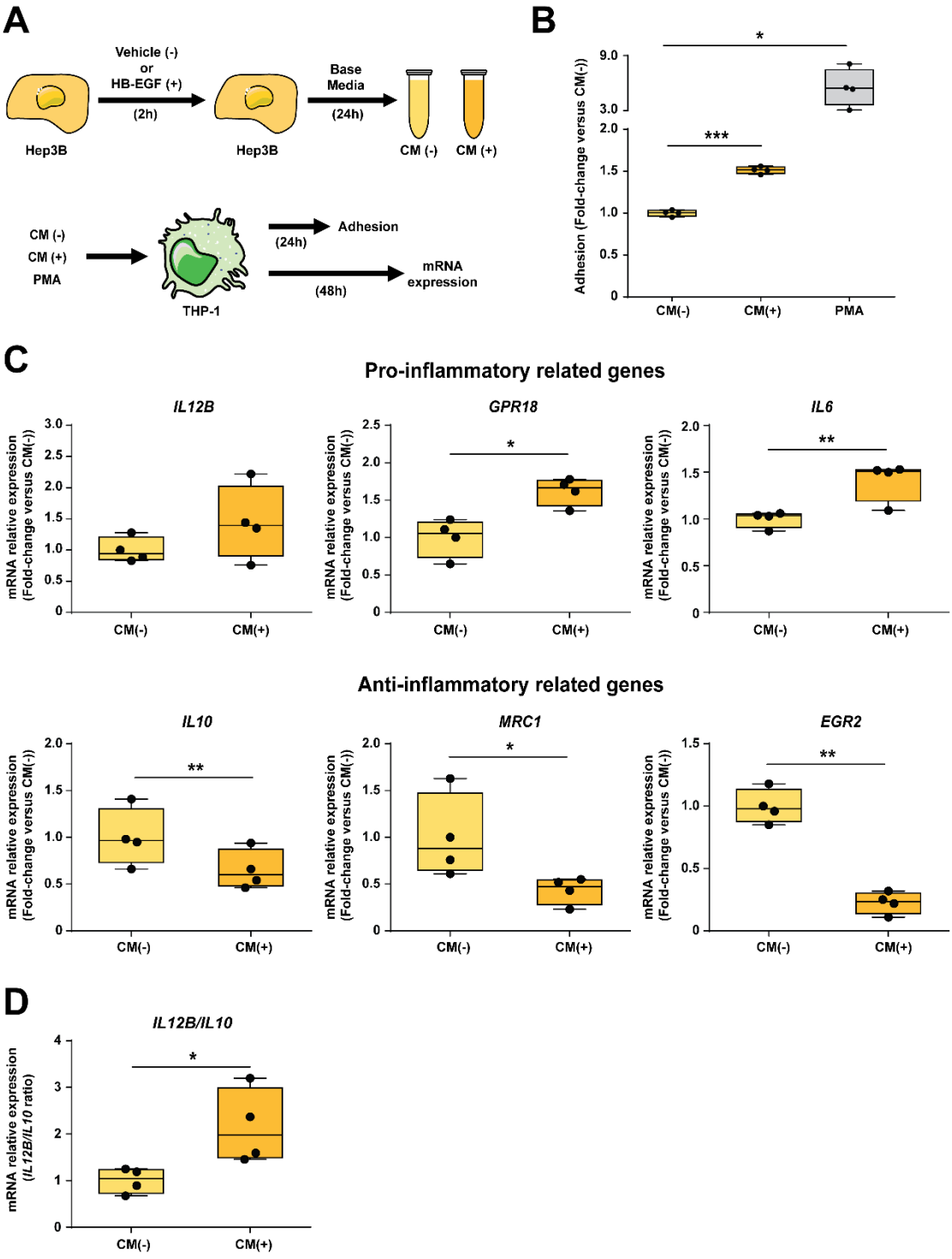

Figure S10. The EGFR pathway regulates the human hepatocyte secretome. Hep3B and THP-1 were used as hepatic and monocyte cell models, respectively. (A) Experimental approach representation. (B–D) Effect of conditioned media (CM) from Hep3B cells treated with (+) or without (−) HB-EGF (20 ng/ml) on (B) THP-1 adhesion, using phorbol myristate acetate (PMA) as a positive control; (C) the expression levels of M1 and M2 associated genes in THP-1 cells assessed using RT-qPCR; (D) *Il12B/Il10* ratio. Data (from at least three independent experiments) are expressed as fold-change versus vehicle: CM(−) from Hep3B cells. *$p < 0.05$, **$p < 0.01$, ***$p < 0.001$ (Student's *t*-test).

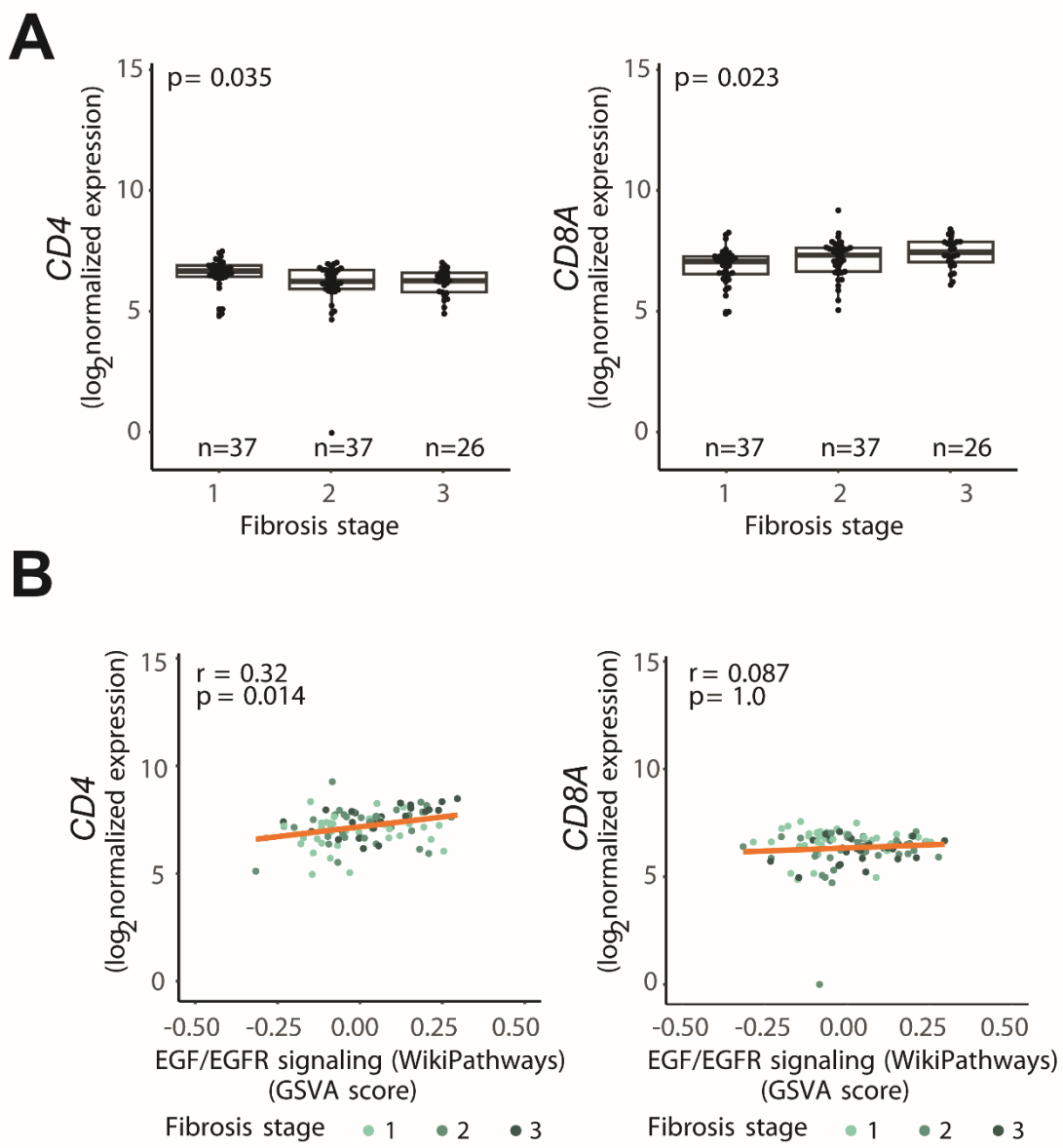

Figure S11. EGFR signaling correlates with changes in lymphocyte populations in human fibrosis. (A) Boxplot of *Cd4* and *Cd8A* across the fibrosis stages. (B) Pearson correlation between the relative enrichment of EGF/EGFR signaling and *Cd4* and *Cd8A* gene expression. Each dot is a sample, and its color indicates the fibrosis stage. Data were analyzed using Kendall's tau test and all *p* values were adjusted for multiple testing.

Supplementary Tables S1–S5

Table S1. Primary antibodies used for immunodetection.

Protein	Antibody	Company	Type	Source	Use	Dilution
α-SMA	ab5694	Abcam, Cambridge, UK	Polyclonal	Rabbit	WB	1/2,000
					IHC	1/50
F4/80	Ab6640	Abcam	Monoclonal	Rat	IHC	1/50
pSMAD3	07-1389	Millipore, Burlington, MA, USA	Polyclonal	Rabbit	WB	1/1,000
SMAD3	04-1035	Millipore	Monoclonal	Rabbit	WB	1/1,000
pEGFR	CST 3777S	CST (Cell Signaling Technology), Danvers, MA, USA	Monoclonal	Rabbit	WB	1/500
EGFR	CST 2232S	CST	Polyclonal	Rabbit	WB	1/1,000
pAkt	CST 4060	CST	Monoclonal	Rabbit	WB	1/1,000
Akt	CST 9272	CST	Polyclonal	Rabbit	WB	1/1,000
pERK	CST 9101	CST	Polyclonal	Rabbit	WB	1/1,000
ERK	CST 4695	CST	Monoclonal	Rabbit	WB	1/1,000
β-Actin	A5441	Sigma-Aldrich, St Louis, MO, USA	Monoclonal	Mouse	WB	1/5,000

WB, western blot; IHC, immunohistochemistry.

Table S2. **Antibodies used for immunodetection of liver immune populations by FACS.**

	Company	Type	Source	Dilution
FITC Rat Anti-Mouse Cd45. Clone I3/2.3	Southern Biotech, Birmingham, AL, USA	IgG	Rat	1/100
APC F4/80 Monoclonal Antibody. Clone BM8	eBioscience, San Diego, CA, USA	IgG2ak	Rat	1/50
PE/Cyanine7 anti-mouse Cd11b(Mac1). Clone M1/70	BioLegend, San Diego, CA, USA	IgG2bk	Rat	1/100
PE/Cyanine7 anti-mouse Cd3. Clone 145-2C11	BioLegend	IgG	Hamster	1/100
PE Rat Anti-Mouse Cd8. Clone 53-6.7	Beckman Coulter, Brea, CA, USA	IgG2ak	Rat	1/50
PerCP/Cyanine5.5 Anti-mouse Cd4. Clone GK1.5	BioLegend	IgG2bk	Rat	1/50
PE anti-mouse Cd206. Clone C068C2	BioLegend	IgG2ak	Rat	1/25
FITC anti-mouse CD25. Clone 7D4	Pharmingen, San Diego, CA, USA	IgMk	Rat	1/25
PE anti-mouse Cd127. Clone A7R34	eBioscience	IgG2ak	Rat	1/25
Brilliant Violet 570 Anti-mouse Cd45. Clone 30-F11	BioLegend	IgG2b	Rat	1/100
PE anti-mouse IL-17A. Clone TC11-18H10.1	BioLegend	IgG1k	Rat	1/25
APC anti-mouse Cd62L. Clone MEL-14	eBioscience	IgG2ak	Rat	1/25
PECy5 anti-mouse Cd44 (SRPD). Clone IM7	BioLegend	IgG1k	Rat	1/25

Table S3. Primers used for RT-qPCR (mouse genes).

Gene	Forward	Reverse
Col1a1	GAGAGGTGAACAAGGTCCCG	AAACCTCTCTCGCCTCTTGC
Col1a1	GAGAGGTGAACAAGGTCCCG	AAACCTCTCTCGCCTCTTGC
Col3a1	GACCAAAAGGTGATGCTGGACAG	CAAGACCTCGTGCTCCAGTTAG
Cyp2b10	AAAGTCCCGTGGCAACTTCC	TTGGCTCAACGACAGCAACT
Cyp2e1	AGGCTGTCAAGGAGGTGCTACT	AAAACCTCCGCACGTCCTTCCA
Loxl1	GAGTGCTATTGCGCTTCCC	GGTTGCCGAAGTCACAGGT
Loxl2	TTCTGCCTGGAGGACACTGAGT	TCGGTGATGTCTATCCACTGGC
Mmp2	GTGGGACAAGAACCAGATCAC	GCATCATCCACGGTTTCAG
Mmp9	CCTGGCTCTCCTGGCTTT	AGCGGTACAAGTATGCCTCTG
Timp1	TGGCATCCTCTTGTTGCTATCACTG	TGAATTTAGCCCTTATGACCAGGTCC
Timp3	GAAGCCTCTGAAAGTCTTTGTGG	ACATCTTGCCTTCATACACGC
Tgfb1	GTCAGACATTCGGGAAGCAG	GCGTATCAGTGGGGGTCA
Tgfb2	TCCCCTCCGAAAATGCCATC	GGAAGACCCTGAACTCTGCC
Tgfb3	TTTGCGGAGGACGGAGTAAC	ACAGTCACCAGCATCTCAGC
Ccn2	AGAACTGTGTACGGAGCGTG	GTGCACCATCTTTGGCAGTG
Pdgfb	CCTGCAAGTGTGAGACAGTAG	GGTGTGCTTAAACTTTCGGTG
Adgre1	TGCACTGACACCACAGACAG	TGCAGACTGAGTTAGGACCAC
Tnf	ACGTCGTAGCAAACCACCAA	ATCGGCTGGCACCACTAGTT
Il1b	CTGGGAAACAACAGTGGTCA	CTGCTCATTCACGAAAAGGG
Il10	CCTTCAGCCAGGTGAAGACT	GGCAACCCAAGTAACCCTTA
Il12b	ATTACTCCGGACGGTTCACG	ACGCCATTCCACATGTCACT
Rpl32	ACAATGTCAAGGAGCTGGAG	TTGGGATTGGTGACTCTGATG

Table S4. Primers used for RT-qPCR (human genes).

Gene	Forward	Reverse
EGFR	GCAAATTCCGAGACGAAGCC	CTGTATTTGCCCTCGGGGTT
GPR18	ACCCAAAGTCAAGGAGAAGTC	GCATCAGGAAAGCGAAACAG
IL6	ACCCCCAATAAATATAGGACTGGA	TTCTCTTTCGTTCCCGGTGG
IL12B	CTTGGACCAGAGCAGTGAGG	GAACCTCGCCTCCTTTGTGA
MRC1	GCAAAGTGGATTACGTGTCTTG	CTGTTATGTCGCTGGCAAATG
EGR2	TTGACCAGATGAACGGAGTG	GCCCATGTAAGTGAAGGTCTG
IL10	TGCCTTCAGCAGAGTGAAGA	GCAACCCAGGTAACCCTTAAA
RPL32	AACGTCAAGGAGCTGGAAG	GGGTTGGTGACTCTGATGG

Table S5. In-house EMT signature genes designed by Fabregat's laboratory.

Acvr1	*Il6*	*Tgfb1i1*
Alx1	*Isl1*	*Tgfb2*
Axin2	*Jag1*	*Tgfb3*
Bambi	*Lef1*	*Tgfbr1*
Bcl9l	*Loxl2*	*Tgfbr2*
Bmp2	*Mdk*	*Tiam1*
Bmp4	*Mtor*	*Twist1*
Bmp7	*Notch1*	*Wwtr1*
Col1a1	*Olfm1*	*Zfp703*
Crb2	*Pdpn*	*Zeb1*
Ctnnb1	*Rgcc*	*Zeb2*
Dab2	*Sdcbp*	*Snai2*
Eng	*Serpinb3d*	*Smad1*
Ezh2	*Smad2*	*Cdh1*
Foxc1	*Smad3*	*Cdh2*
Gcnt2	*Smad4*	*Vim*
Glipr2	*Snai1*	*Krt18*
Hdac2	*Tcf7l2*	*Cxcr4*
Il1b	*Tgfb1*	*Smn1*